Contribution of Entanglements to the Mechanical Properties of Carbon Black Filled Polymer Networks

G. Heinrich*

Continental AG, Materials Research/Tire Research, P.O. Box 169, D-3000 Hannover, FRG

T. A. Vilgis

Max-Planck-Institut für Polymerforschung, P.O. Box 3148, D-6500 Mainz, FRG

Received August 17, 1992; Revised Manuscript Received November 9, 1992

ABSTRACT: A rigorous molecular statistical model of filled polymer networks with quenched structural disorder coming from the conventional chemical cross-links between polymers and from an ensemble of rigid and highly dispersed multifunctional filler domains is presented. Specific surface and structure of the filler and its effect of "hydrodynamic" disturbance of intrinsic strain distribution are explicitly taken into account. The conformational constraints (entanglements, packing effects) of polymer chains in the mobile rubber phase are described by a mean-field-like tube model. The calculation of the elastic free energy follows a straightforward generalization of the non-Gibbsian statistical mechanics using the replica technique. Within the model proposed, the network is characterized by four typical length scales: the Kuhn's statistical segment length l_s of the polymers; the root-mean-square end-to-end distance of the mobile network chains R_c; the square root b_{PR} of the average area available to a couple site between mobile polymer phase and filler surface; and the lateral tube dimension d_o, which is equal to the mean spacing between two successive entanglements in the mobile rubber phase. Application of the theory to stress–strain experiments of unfilled and carbon black filled vulcanizates (styrene–butadiene copolymer rubbers, butadiene rubbers) yields the characteristic length scales R_c, b_{PR}, and d_o. The typical relations $b_{PR} \approx l_s$ and $l_s < d_o < R_c$ were found. The estimated values of the entanglement spacing d_o agree with independent calculations for unfilled systems and direct (neutron scattering) measurements. It is further found that the contribution of entanglements to the equilibrium modulus of the elastomer is in the order of contributions coming from the polymer–polymer and polymer–filler junctions. The observation that the entanglement contribution to the elastic modulus decreases somewhat with increasing filler content (i.e., d_o increases) is discussed within scaling considerations. It is concluded that the estimated coupling density between polymer phase and carbon black surface is related to the mean number of entanglements formed between the tightly adsorbed bound rubber and the bulk rubber. The problem of polymer adsorption on a carbon black surface is discussed within the concept of disorder-induced localization of polymers on disordered or fractal surfaces.

1. Introduction

A still controversial question on the mechanical behavior of rubber elastic solids is whether topological constraints, such as chain entanglements, contribute to the elastic properties of carbon black filled elastomers and, if so, to what extent. This discussion is strongly coupled with the success of formulating a well-founded molecular statistical theory of such systems.

It is noticed that—in contrast to filled networks—the molecular statistical basis of unfilled cross-linked and entangled polymer networks is conceptionally established. Kästner,[1] Ronca and Allegra,[2] and Flory and Erman[3] derived the model of restricted junction fluctuations by assuming that fluctuations of the network junctions about their mean positions are restricted by topological interactions. This theory contains the assumption that the restricted-phase space (due to entanglements) available to the chains has its only effect on the fluctuations of cross-links; i.e., the model does not account for local restrictions. However, a wealth of experimental evidence clearly demonstrates the importance of the configurational restrictions of the whole network chains to explain the mechanical behavior of the cross-linked network.[4-11] In the corresponding molecular models, it is assumed that entanglements act along the entire contour length of a network strand, either discretely or continuously in a mean field manner. In the former case, the restricting effects of entanglements on the lateral motion of chains are modeled by pointlike constraints between junctions (modified constrained junction model)[12] or slip-links and hoops.[13-20] In the latter case, configurational tubes have been introduced successfully which have their origin in studies of the dynamics of long polymer molecules in melts.[6,19,21] In rubbers the tube becomes frozen due to quenching by cross-links, which preserves the local topology. These models have been discussed extensively elsewhere.[6,7,19]

Of several versions of the entanglement models, the most empirically successful seems to be the tube model. Recent results obtained by using such mean field tube models for the determination of network parameters of a set of styrene–butadiene rubber samples led to the conclusion that a reliable theoretical basis for the treatment of stress–strain data for unfilled rubber elastic networks is available.[9,10] It was shown that the tube model allows a proper separation of cross-links and constraint contribution to the stress–strain behavior and a reliable determination of cross-link densities.[6,9,10]

The physical situation changes dramatically in the case of filled polymer networks. It was realized early that carbon black contributes as the most important active filler in rubbers and it became one of the most important components in the manufacturing of rubber products, with a consumption second only to the polymer itself.

A carbon black filled elastomer should be regarded as a composite characterized by a "rubbery" continuous phase and a particulate "rigid" dispersed phase. When carbon black is dispersed in the rubber, substantial changes are observed in the tensile properties and the dynamic mechanical properties of the compound compared to the pure unfilled rubber. A large amount of work has been published discussing the role of carbon black in rubber

0024-9297/93/2226-1109$04.00/0

compounds, and the reader is referred especially to refs 22–27 for some important details. Many of the proposed approaches, although they allowed significant progress in the technology, were based on empirical or semiempirical testing methodologies.

The main objective of this article is to elucidate the role of entanglements and to estimate their contribution in terms of tubelike configurational constraints in carbon black filled networks in thermodynamical equilibrium. The paper is therefore divided into two parts. In the first part, a general theory of filled rubbers is presented in which a well-founded separation of cross-link and constraint contributions to the stress–strain behavior can be achieved by generalizing and combining recent theoretical results resting on the non-Gibbsian statistical mechanics applied to polymer networks[28] and on the configurational tube approach.[6] The influence of filler particles is described by their hydrodynamic effect together with its action as an ensemble of highly dispersed multifunctional domains. This theory is a general one, and the specific problem of carbon black filled rubbers is one of the most important examples. Among the other possible fillers which are suitable for the discussion of the theory, only silicia give effects and substantial reinforcement, compared with the effect of carbon black. In the second part, the application of the theory to stress–strain measurements of carbon black filled rubbers of different types of polymers is performed. In this case, the "occluded rubber" effect is, additionally, taken into account. It is defined as the polymer that penetrated the void space of the individual carbon aggregates, partially shielding it from deformation.[24,29] The introduction of a coupling between the mobile rubber phase and active filler domains to explain the enhancement of vulcanizate properties is based on the experimental experience that the network modulus is higher than that predicted from the pure hydrodynamic interaction model.[26,30] We will discuss later that this coupling together with the additional reinforcement is caused by entanglements formed between tightly adsorbed bound rubber on the filler surface and the bulk rubber far removed from the surface. We will argue, for the first time, that (besides covalent bonds between bound rubber molecules and filler (carbon black) surface) disorder-induced localization on the disordered or even fractal surface plays an important role in understanding bound rubber attachment.

2. Theoretical Section

2.1. General Theory. Filled rubberlike networks are special disordered systems in which several levels of disorder are present. Each demands a different treatment. Small-scale disorder on the level of the monomeric units of the polymers is absorbed as usual into the random flight statistics of the Gaussian chain model via the Kuhn length. The basic characteristics of the unfilled networks are the large-scale topology of cross-link connectivity and the topology of trapped entanglements. Both types of large-scale topology are fixed by the cross-links. The special case of carbon black filled rubbers obeys an additional transient large-scale topology of filler when the carbon black content is roughly above 10 parts per 100 parts rubber. Carbon black consists then of irregular, branched aggregates of firmly fused nodular subunits. These aggregates are "interacting" in order to form agglomerates. The dispersed carbon black agglomerates form a network themselves in the polymeric media. This carbon black network is hold tight by van der Waals forces, and its connectivity is, however, sensitive to strain and temperature. After 6–7% strain it is completely disrupted and broken in discontinuous pieces of clusters that interfere with the polymer matrix primarily by hindering the mobility of the polymer chains.[31]

It is clearly impossible to treat all these complex phenomena within a well-defined molecular statistical model without any approximations.[26] Therefore, we use a simplified mean field approach and consider a generalized configurational tube model in which the network chains are connected through the conventional chemical junction points (in our case, sulfur bridges between the primary molecules) and, additionally, through an ensemble of rigid and highly dispersed multifunctional filler domains.[28,32]

Let us now discuss the configurational partition function of this general model and briefly sketch the calculation of the elastic free energy. In the first step we derive the phantom network-like contribution to the free energy; i.e., we neglect topological constraints of the rubber phase which will be added later. To derive the elastic free energy, one can follow the representation of the non-Gibbsian formula for quenched systems in the replica formulation.[33] The replica technique is known to be the most powerful tool in the statistical mechanics of systems with quenched disorder.[34] For technical details the reader is referred to the extensive paper by Deam and Edwards.[33] When this technique is followed, the cross-link constraint becomes simple to handle, if the network is represented by a huge chain of contour length $L = NL'$, where N is the number of primary chains of length L'. The observable (macroscopic) free energy becomes

$$F = -k_B T \lim_{n\to 0} \frac{\partial}{\partial n} \log Z(n) \tag{1}$$

where $Z(n)$ is the generalized replicated partition function

$$Z(n) = \int\int \cdots D_w[\mathbf{R}^{(\alpha)}(s)]\{[\int_0^L ds_1 \int_0^L ds_2 \prod_{\alpha=0}^{n} \delta(\mathbf{R}^{(\alpha)}(s_1) - \mathbf{R}^{(\alpha)}(s_2))]^{M_c}[\int_0^L ds_1 \int_0^L ds_2 \cdots \times \int_0^L ds_{f_F/2} \prod_{\alpha=0}^{n} \int_{V^{(\alpha)}} d\mathbf{R}_c^{(\alpha)} \prod_{i=1}^{f_F/2} g_i^{(\alpha)}(\mathbf{R}_i^{(\alpha)}(s_i) - \mathbf{R}_c^{(\alpha)})]^{M_f}\} \tag{2}$$

Here, α is the replica index ($0 \le \alpha \le n$), $V^{(\alpha\neq 0)}$ is the deformed sample volume, and $V^{(\alpha=0)}$ is the volume of the sample in the undeformed reference state. The partition function given in eq 2 accounts for the fact that the probability distribution of the network is given by the constraint averaged over the Gaussian chain configurations. The corresponding probability is given by the Wiener measure, which, in $3(n+1)$ dimensions in replica space, takes the form

$$D_w[\mathbf{R}^{(\alpha)}(s)] = \exp\left\{-\frac{3}{2l_s}\sum_{\alpha=0}^{n}\int_0^L \left(\frac{\partial \mathbf{R}^{(\alpha)}(s)}{\partial s}\right)^2 ds\right\} \prod_{\alpha=0}^{n} \delta\mathbf{R}^{(\alpha)}(s) \tag{3}$$

Here, l_s denotes the Kuhn's statistical segment length. The network is represented by a huge chain internally cross-linked at M_c cross-linking points where it touches and at the surfaces of M_f filler particles. The pointlike local cross-link constraints are easy to handle and can be represented by[33]

$$[\int_0^L \int_0^L ds_1\, ds_2\, \delta(\mathbf{R}(s_1) - \mathbf{R}(s_2))]^{M_c} \tag{4}$$

The δ-function makes sure that if two segments s_1 and s_2 meet on the huge network chain they can form a permanent

constraint $\mathbf{R}(s_1) = \mathbf{R}(s_2)$. Hence, this process will produce a network junction of functionality $f_N = 4$.

The constraints due to M_f filler particles are somewhat more complicated to mimick analytically. A crude model is to assume solid spheres of an average functionality $f_F \gg f_N$ (=4). If a filler fixes segment s_i to segment s_j, another couple between the vector positions $\mathbf{R}(s_i)$, $\mathbf{R}(s_j)$ and the center of the particle, $\mathbf{R}_c$, has been produced. Graphically it can be represented by the following diagrams:

for $f_F = 4$

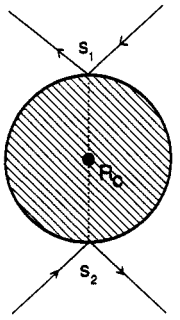

for $f_F = 6$

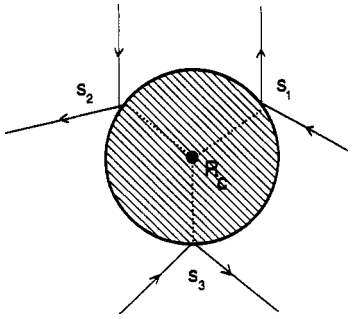

and so forth.

These "filler constraints" are crudely represented by a Gaussian potential

$$g_i(\mathbf{R}_i(s_i) - \mathbf{R}_c) = \prod_{\mu=x,y,z} \left(\frac{2}{\pi\epsilon_\mu^2}\right)^{1/2} \exp\left\{-\frac{2}{\epsilon_\mu^2}(R_{i\mu}(s_i) - R_{c\mu})^2\right\} \quad (5)$$

where we have assumed that the average Cartesian component of the distance between particle center $\mathbf{R}_c$ and vector position $\mathbf{R}_i(s_i)$ is given by $\epsilon_\mu/2$. The quantity ϵ_μ is a typical linear extension of a filler particle. We have to note that this model of filler constraints does not specify the nature (physically or covalent) of the contacts between polymer and filler surface. This point will be discussed later in more detail. Although we have assumed solid incompressible filler particles, we may introduce a general deformation dependence of the filler domains; i.e.

$$\epsilon_\mu = \epsilon\xi(\sigma_w; E_f) \quad (6)$$

Here, $\xi(...)$ is an unspecified function and σ_w the true mechanical stress which deforms the macroscopic sample. E_f denotes the elastic modulus of the filler. We will not discuss this here but leave it for a separate paper, where ξ can, for example, be specified by a linear Hookean law between ϵ_μ and $(\sigma_w)_\mu$. The elastic free energy itself becomes then a function of the elastic force, which can be determined from a resulting differential equation after deriving the free energy.[32] Throughout the present paper the carbon black filler is assumed to consist of solid particles which cannot be deformed, i.e., $\epsilon_\mu = \epsilon$. This is to settle some basic features of the system.

It is important to note at this point that the partition function eq 2 is the simplest formulation of filled phantom networks which uses chain variables $\mathbf{R}(s)$ directly. It assumes the chains are Gaussian; the cross-links *and* filler particles are placed in position randomly and instaneously and are thereafter permanent. Constraints arising from entanglements and packing effects will be introduced later using the mean field approach of harmonic pipe constraints.

To handle the constraint term mathematically, it is usually expressed in terms of a fugacity or a chemical potential via the identity

$$X^N = \frac{1}{2\pi i}\oint_C \frac{d\mu N!}{\mu^{N+1}} e^{\mu X} \quad (7)$$

where the contour C encloses the origin. The generalized partition function then takes the form

$$Z(n) = \int \prod_\alpha \delta R^{(\alpha)} \oint_C \frac{d\mu_c M_c!}{2\pi i \mu_c^{M_c}} \oint_C \frac{d\mu_f M_f!}{2\pi i \mu_f^{M_f}} \times \exp\left\{-\frac{3}{2l_s^2}\sum_{\alpha=0}^{n}\int_0^L \left(\frac{\partial \mathbf{R}^{(\alpha)}(s)}{\partial s}\right)^2 ds + Q^*\right\} \quad (8a)$$

$$Q^* = \mu_c \int_0^L ds_1 \int_0^L ds_2 \prod_{\alpha=0}^{n} \delta(\mathbf{R}^{(\alpha)}(s_1) - \mathbf{R}^{(\alpha)}(s_2)) + \mu_f \int_0^L ds_1 \cdots \int_0^L ds_k \prod_{\alpha=0}^{n} \int_{V^{(\alpha)}} d\mathbf{R}_c^{(\alpha)} \prod_{i=1}^{k} g_i^{(\alpha)}(\mathbf{R}_i^{(\alpha)}(s_i) - \mathbf{R}_c^{(\alpha)}) \quad (8b)$$

where $k = f_F/2$.

The evaluation of $Z(n)$ will be done along the lines of Edwards and Deam for unfilled networks, who used a Feynman variational principal.[33] We briefly sketch the main steps in our case of filler-containing networks in the Appendix. The rigorous derivation of the elastic free energy leads to the following expression:

$$F = \frac{1}{2}k_B T(M_c + g_f M_f)\sum_\mu \lambda_\mu^2 + \text{terms independent of deformation} \quad (9)$$

where $g_f \equiv k - 1$.

Equation 9 is nothing but the free energy of a phantom network consisting of $M_c + g_f M_f \approx M_c + kM_f$ (for k large) cross-links. The deformation-independent terms contain the two localization parameters w^c and w^f of the polymer–polymer junctions and polymer–filler couples, respectively (Appendix, eqs A.21 and A.22). Both quantities have been introduced as the strength of harmonic trial potentials which simulate the configurational restrictions due to the cross-links. The inverse of a localization parameter defines the mean distance in which the cross-links are localized; i.e., it is proportional to the mean square radius of gyration of a segment between two cross-links. This surprisingly simple but physically clear result (eq 9) for filled elastomers was intuitively originated by Bueche.[35] Here, we have given a derivation based on arguments of statistical thermodynamics. Note that eq 9 generalizes to additional deformation-dependent terms when a deformation dependence of filler domains is assumed, as in eq 6 proposed.[32]

The theoretical concept used in our model now offers a clear route for including entanglement constraints and

packing effects. There are various ways of including such restrictions, and they have been discussed exhaustively by Vilgis[7] and Edwards and Vilgis.[19] As already discussed in the Introduction, simple and successful mean field models are based on the configurational tube picture. Its harmonic pipe approach has been investigated by Heinrich et al. using the basic assumption that the chains do not have free access to the total space between the cross-links but are trapped in a cage due to the topological restrictions.[6,36,37] The physical basis of the tube approach to the contribution of entanglement and packing effects to rubber elasticity is the large degree of coil interpenetration. In this case, the relation $N_F \gg 1$ holds, where N_F is the Flory number.[64] It is equal to the number of network chains within a coil volume of one chain. For $N_F \gg 1$, the restrictions on the configurations of one chain under consideration are strong and are caused by contributions of a number of chains of the order of N_F. Consequently, it may be expected that the fluctuations of the topological constraints are small and the effects of large-scale correlations are screened out so that the topological constraints are well described by a constraining potential. This picture was suggested first by Edwards.[38] Any tagged chain is confined to the neighborhood of the initial or mean configuration by a restoring (usually harmonic) potential. Following the usual rules of statistical mechanics, this confining potential has to be determined self-consistently.[36,37] In the case of $N_F \gg 1$, it is reasonable to assume that the contributions to the confining potential are not controlled by the global topology of all chains in the coil volume but entirely by the local topology of the chains in the neighborhood of the chain under consideration. Strength and deformation dependence of the constraints may be expressed in the case of tube models in a very instructive way by the square root of the mean square deviation of the position of a segment, $\mathbf{R}(s)$, from its average position $\mathcal{R}(s)$: $d_\mu = \langle (R_\mu(s) - \mathcal{R}_\mu(s))^2 \rangle^{1/2}$. In deformed systems, it is preferable to work in the reference system of the principal axes, where the deformation tensor is diagonal and to use the components d_μ of the mean square deviations in the directions of the principal axes. The deformation dependence of the tube parameter was derived in refs 36 and 37, leading to the following power law:

$$d_\mu = d_o \lambda_\mu^{\nu} \tag{10}$$

with $\nu = 1/2$. This "loss of affiness" of the tube dimension was explained by the following mechanism: after the sample is stretched, the tube axis experiences an affine displacement followed by the first relaxation process according to the Doi–Edwards terminology.[39] As a result of this process, parts of the chain of the order of tube dimension are in equilibrium; i.e., their free energy does not change relative to the undeformed state. This was taken into consideration in the calculations by introducing an effective number of degrees of freedom for the constraining chains. In ref 6 the exponent ν in eq 10 was replaced by $\beta\nu$ ($0 \le \beta \le 1$). The parameter β was introduced to allow for the strong swelling dependence of the constraints. β can be considered as an empirical parameter which describes the relaxation of the deformed tube in the deformed state to an undeformed tube corresponding to the equilibrium state. In the following, we use the value $\beta = 1$, i.e., relevant for almost complete converted dry networks made from long primary chains and cross-linked highly so that the molecular mass of a strand is much smaller than the molecular mass of the primary chains.[6]

The tube model generalizes the above discussed phantom network localization parameter w_μ^c (eq A.21) into which the tube parameter now enters:[6]

$$(w_\mu^c)^2 \rightarrow (\tilde{w}_\mu^c)^2 + \frac{6}{d_\mu^4} \tag{11}$$

with

$$\tilde{w}_\mu^c \approx \frac{6M_c}{l_s L}\left\{1 + \left(1 + \left(\frac{6M_c}{l_s L} d_\mu^2\right)^{-2}\right)^{1/2}\right\}^{1/2} \tag{12}$$

The localization strength w_μ^c in eq A.22 is related to a quadratic potential with the meaning that the chain is localized by chemical cross-links alone. The modified localization parameter (eq 11) contains additional contributions coming from the configurational tube by its average lateral dimension d_μ. In the case of slightly and moderately cross-linked networks ($M_c/N = M_c L'/L \simeq 1$), we have strong topological constraints $l_s L_c / d_\mu^2 \gg l^6$ (L_c is the contour length of a network chain with both ends fixed in cross-links). Thus the following expression is obtained:

$$\tilde{w}_\mu^c \approx \left(\frac{6M_c}{l_s L}\right)^{1/2} \frac{1}{d_\mu} \tag{13a}$$

$$(\tilde{w}_\mu^c)^2 + \frac{6}{d_\mu^4} \simeq \frac{6}{d_\mu^4}\left(1 + d_\mu^2 \frac{M_c}{l_s L}\right) = \frac{6}{d_\mu^4}\left(1 + \frac{1}{2}\frac{d_\mu^2}{l_s L_c}\right) \approx \frac{6}{d_\mu^4} \tag{13b}$$

The deformation dependence of the tube radius d_μ (eq 10) leads then to an additional deformation-dependent contribution in the elastic free energy:[6]

$$^1/_2 k_B T N_c \sum_\mu (d_o/d_\mu)^2 \tag{14}$$

where N_c is the number of network chains and d_o the undeformed tube parameter.

Equations 9, 11, and 14 yield the following uniaxial ($\lambda_x = \lambda$, $\lambda_y = \lambda_z = \lambda^{-1/2}$) stress–strain relations, which consist of two contributions:

$$\sigma_M(\lambda) = \sigma/(\lambda - \lambda^{-2}) = G_c(\varphi) + G_e(\varphi) f(\lambda) \tag{15a}$$

$$f(\lambda) = \frac{2}{\beta}\frac{\lambda^{\beta/2} - \lambda^{-\beta}}{\lambda^2 - \lambda^{-1}}, \quad f(\lambda{=}1) = 1 \tag{15b}$$

$$G_c(\varphi) = G_c(1 - \varphi) + k_B T \nu_f \varphi \tag{15c}$$

where σ_M is the Mooney stress, σ is the nominal stress, λ is the macroscopic strain ratio, and φ is the filler volume fraction, with

$$G_c = \rho_p RT/M_c \tag{16}$$

$$G_e(\varphi) = \frac{1}{4(6)^{1/2}} k_B T n_s l_s^2 / d_o^2(\varphi) \tag{17}$$

where ρ_p is the polymer density, n_s is the polymer segment number density, R is the gas constant, and k_B is the Boltzmann constant.

The φ-dependence of the constraint modulus $G_e(\varphi)$ is related to the φ-dependence of the tube parameter and will be discussed later.

The shear modulus $G_c \equiv G_c(\varphi{=}0)$ of the corresponding unfilled network is related purely to the polymer–polymer junctions. The elastically effective number density (re-

lated to the filler volume) of polymer–filler contacts is denoted by ν_f. This quantity gives no information about the nature (physical or chemical) of the bond. Obviously, optimal carbon black reinforcement appears to involve both physical and chemical interaction.[27]

The second part of eq 15 stems from the polymer–polymer entanglements. Their contribution to the modulus $G_e(\varphi)$ depends on the filler concentration in networks.

2.2. Specification and Discussion. It has to be realized that in the case of filled rubbers the deformation λ appropriate to the rubber matrix should be replaced by the intrinsic tension ratio λ'. In this way, the pure hydrodynamic effects of the filler particles, i.e., the disturbance of strain distribution, are taken into account:

$$\lambda' = (\lambda - 1)x_{eff} + 1 \tag{18}$$

The effective Guth–Gold amplification factor is[22,23]

$$x_{eff} = 1 + 2.5\varphi_{eff} + 14.1\varphi_{eff}^2 \tag{19}$$

and contains the effective filler volume fraction, φ_{eff}, which is larger than the volume loading φ calculated from the weight loading and density of filler. Although several other calculations of the second-order term in eq 19 found a considerably lower value,[65] we used the coefficient 14.1, which is commonly used in rubber technology. The difference between φ and φ_{eff} is a specific property of carbon black fillers and is explained empirically by the complex architecture of the carbon black aggregates. The aggregates obey a substantial portion of internal volume which can be filled with polymers. The rubber internal to the aggregates, the occluded rubber, can be effectively shielded from the strains–stresses experienced by the bulk rubber. Thus, the amount of rubber bearing the stresses imposed upon the sample is reduced by the amount of rubber internal to the aggregates. An equivalent statement is that the carbon black aggregates behave as if their total volume is the solid volume, calculated from the weight and density, plus the internal volume filled by rubber. It is further assumed that parts of the occluded polymer volume will be again elastically active under conditions of high strain. This leads to a reducing of the occluded volume. This occluded rubber concept has been proposed by Medalia and can be summarized by the following empirical relation:[24,29]

$$\varphi_{eff} = \varphi(1 + 0.5[(1 + 0.02139\Gamma_{DBP})0.685 - 1]) \tag{20}$$

where Γ_{DBP} is the DBP (dibutyl phthalate) adsorption number in $cm^3/100$ g which serves as an empirical measure for carbon black structure in rubber and carbon black technology. Kraus proposed a similar empirical model based on arguments on the relation of strain and nonaffine deformation.[22]

Coming back to the result eq 15 derived here, we note that the quantities $G_c(\varphi)$ and $G_e(\varphi)$ are determined by a linear least-squares fit of the Mooney plot (σ_M vs $f(\lambda')$) operating in the strain regime before the onset of the stress upturn at larger deformation. Each of the curves shows a linear relation over a range of low and moderate extension, having an intercept on the axis $f(\lambda') = 1$ of G_c and a slope of G_e. The quantity ν_f can be obtained from the chemical moduli G_c when the stress–strain data of the unfilled and the corresponding filled rubber samples are compared:

$$\frac{G_c(\varphi)}{G_c} = (1 - \varphi) + \frac{k_B T \nu_f \varphi}{G_c} \tag{21}$$

The coupling density ν_f is related to the average area A_{PR} which is available to a coupling site between mobile rubber phase and filler surface:

$$A_{PR} \equiv b_{PR}^2 = A_R \rho_R / \nu_f \tag{22}$$

where b_{PR} is a typical length scale of the coupling problem. ρ_R is the density of filler (=1.7 g/cm^3 for carbon black). A_R is the specific surface area of the filler (in units of m^2/g).

The modulus G_e in eq 15 represents the constraint contribution which is proportional to the plateau modulus G_N^0 of the un-cross-linked bulk polymer.[6] Graessley and Edwards proposed that the plateau modulus should be determined solely from the density of chain contour length and the statistical segment length.[40] Dimensional arguments lead to the relationship

$$G_N^0 \sim n_s^a \tag{23}$$

where n_s is the segment number density. The exponent a was determined from experiment to be in the range $2 \le a \le 2.3$. Various scaling pictures of polymer entanglement yield various exponents a (=2, $^7/_3$, 3) as has been recently discussed by Colby et al.[41] A recent compilation of melt data indicates $a = 2.67$.[42]

The relation between constraint modulus and tube parameter leads to the power law dependence

$$d_0 = \alpha(n_s l_s^3)^{(1-a)/2} l_s \tag{24}$$

Recent calculations on polymer melts, based on a mean field model for entanglements and packing effects, led to eq 24 with $a = 2$ and $\alpha = \alpha_{melt} \approx 8.5$,[36,37,43] whereas small-angle neutron-scattering results favor both the packing model and the Graessley–Edwards scaling picture.[44] The value of the prefactor α_{melt} is almost identical to the value obtained by a least squares fit of experimental data in the Graessley–Edwards paper.[40] However, α could not be calculated with the necessary accuracy in the network case (the calculations gave $\alpha \approx 1$).[37] Therefore, α was determined by comparing theoretical results for the constraint contribution G_e with experimental values for some typical elastomers (natural rubber, polybutadiene, poly(dimethylsiloxane)).[6,45] We use the stress–strain results of this paper to estimate α_{nw} from the relationship[6]

$$\alpha_{nw} = 3.04(G_N^0/G_e)^{1/2} \tag{25}$$

Equations 16, 22, 24, and 25 yield three typical length scales of the filled network: the root-mean-square end-to-end distance of the mobile network chains R_c (which is related to the average molecular mass of these chains); the square root b_{PR} of the average area available to a couple site between polymer and filler; and the lateral tube dimension d_0, which is equal to the mean spacing between two successive entanglements in the mobile rubber phase.

So far, the proposed theory of filled rubbers was specified to the case of carbon black filler. Among other possible fillers which are suitable for the discussion of the present theory, only silicia give substantial reinforcement, compared with the effects of carbon black. Silicia particles are amorphous in structure and their surface is irregular, but unlike carbon black, the surface is polar, a property which is excluded in the theory.

3. Experimental Section

3.1. Rubbers and Experimental Procedure. The polymers chosen were high *cis*-1,4-polybutadiene (Buna CB 10) and two types of styrene–butadiene copolymers: (i) emulsion SBR with 40% styrene (SBR 1516); (ii) solution SBR with 23% styrene, 15% 1,4-*trans*-butadiene, 11% 1,4-*cis*-butadiene, and 51% 1,2-butadiene. The filled test samples were prepared as follows: The ingredients

Table I
Data of Raw Polymers and Compounds[a]

	cb content (phr)	T_g (°C)	ML (1+3) (units)	t_{95} (min)
polybutadiene	0	−101	46	15
	50		100	5
styrene–butadiene copolymer	0	−28	43	90
	50		74	70
high vinyl SBR	0	−18	51	96
	50		85	65

[a] cb, carbon black; T_g, DSC glass transition temperature (heating rate 20 K/min); ML, Mooney viscosity (150 °C); t_{95}, optimal curing time.

(100 parts per hundred rubber (phr) oil-free polymer, 50 phr HAF carbon black N 339 (ASTM designation) with $A_R = 96\ m^2/g$ and $\Gamma_{DBP} = 120\ cm^3/100\ g$, and 5 phr aromatic oil, semiefficient vulcanization system) of the compound were mixed on a two-roll mill, molded, and cured at 150 °C for a specified time (t_{95}) ensuring optimum cure. Additionally, the corresponding unfilled samples were prepared. The cure times, glass transition temperatures of the raw polymers, and Mooney viscosities of the uncured compounds are given in Table I. All dogbone samples were cut from sheets of vulcanized rubber, ~1.5 mm thick. The tensile tests were performed with a Monsanto tensile tester at 25 °C using low deformation rates $\dot{\epsilon} = 0.0025\ s^{-1}$. The stress–strain curves were estimated for three different samples of a given sheet. Then, the averages of the corresponding three data points were estimated (standard deviations 0.01–0.05). The moduli G_c and G_e were determined from the linear part of moderate deformation in the generalized Mooney plot σ_M vs $f(\lambda')$ according to eq 15 (Figure 1). Plateau modulus data of the utilized polymers were taken from ref 47. More details of the experimental procedure are given in ref 61.

Although the used deformation rate was extremely slow, dynamic contributions to the stress are nonvanishing and will be discussed here. A reduction to equilibrium can be performed with the method proposed and described in refs 9 and 48, where separability of strain and time dependence of the stress data (SBR 1500 samples, $\dot{\epsilon} \sim 10^{-3}\ s^{-1}$) according to eq 15 has been assumed. It could be shown in these papers that only for low cross-linking densities (or M_c larger than 10^4 g/mol) the additional assumption of simultaneous relaxation of cross-link and constraint contributions to the tensile force leads to cross-link densities from 10% to 20% lower than the values without corrections and to negligible effects for d_o. The assumption of the relaxation of the constraint contribution alone causes negligible effects for the calculated cross-link densities and, therefore, reproduces the result for the typical length scales in unfilled and filled rubbers without corrections of the dynamical contributions. Clearly, measurements with varying deformation rates should be performed in future for a larger variety of cross-linked polymers.

3.2. Results and Discussion. The values estimated for the moduli G_c and G_e and the corresponding values of the coupling density polymer–filler ν_f are given in Table II. The estimated (eq 22) values of an average area A_{PR}, which is available to an elastically effective polymer–carbon black couple on the filler surface, approximately agree with stress–strain investigations using a different model of carbon black reinforcement.[48]

The average molecular mass of the network chains (Table II) is related to G_c according to the relation $M_c = \rho_P RT/G_c$, where ρ_P is polymer density. The decrease of

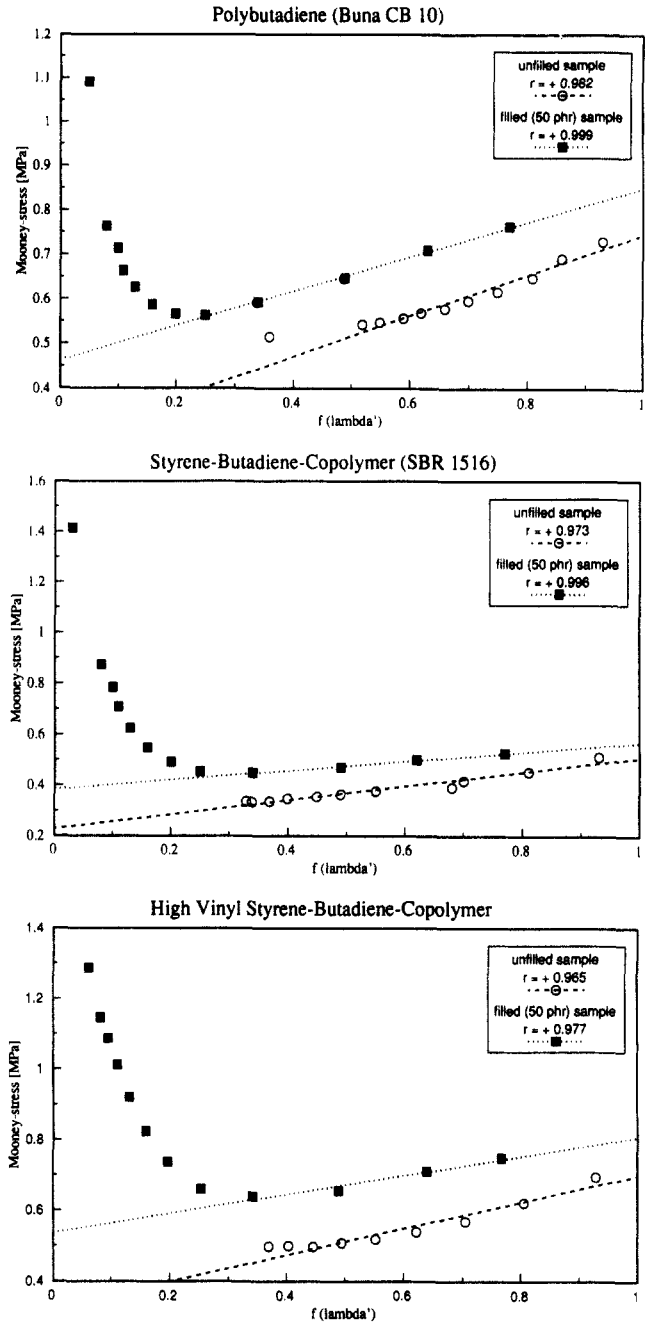

Figure 1. Mooney stress (eq 15) vs deformation function f of the tubelike contribution to the tensile force. The function f contains the strain amplification factor.

M_c with increasing carbon black content is equivalent to an increase in the formation of polymer–filler couples and short bridging chains between filler particles which enlarge the extension of the filled network or of highly bounded clusters of filler particles. A slightly different interpretation is given in ref 48, where the increase of cross-linking density and the formation of bridging chains in filled rubbers is related to a rescaling of the filler volume fraction.

The observation that the entanglement modulus G_e decreases slightly in the filled network is explained as follows: With increasing filler content, the network chains become shorter and the number of entanglements between two cross-links decreases. Moreover, the chains are more aligned upon stretching, as in the unfilled case. For shorter chains the configurational constraints become less effective in comparison to effects of limited chain extensibility; i.e., G_e decreases.[62] This decrease leads to a slight increase of d_o.

Table II
Typical Parameters of Unfilled and Filled Networks Estimated from Uniaxial Tensile Tests[a]

rubber	cb content (phr)	G_c (MPa)	G_e (MPa)	M_c (g/mol)	$10^{-20}\nu_f$ (cm^{-3})	A_{PR} (nm^2)	α_{nw}	$d_{nw}(50)/d_{nw}(0)$	d_{melt}/d_{nw}
polybutadiene	0	0.278	0.460	8481					2.17
							3.92	1.04	
	50	0.461	0.391	5280	1.78	0.9			2.08
styrene–butadiene copolymer	0	0.226	0.286	10770					1.60
							5.34	1.12	
	50	0.383	0.184	6355	1.60	1.0			1.43
high vinyl styrene–butadiene copolymer	0	0.325	0.371	7489					2.0
							4.30	1.08	
	50	0.537	0.269	4533	2.21	0.7			1.85

[a] cb, carbon black; G_c,G_e, contributions of chemical cross-links and entanglements, respectively, in the rubber phase to the shear modulus; M_c, molecular mass of network chains; ν_v, density of couples (related to the filler volume) between rubber phase and filler; A_{PR}, average area (related to the carbon black surface) available to a couple; α_{nw}, prefactors in the relations between tube diameters (d_{nw}, d_{melt}) and segment number density.

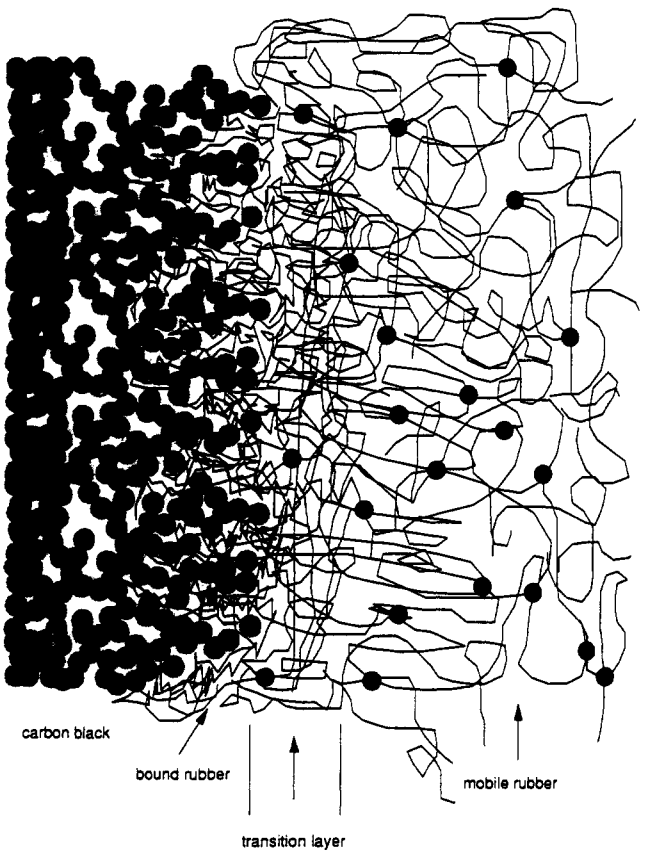

Figure 2. Sketch of the entangled bound rubber–mobile rubber model.

We have to note that results found from stress–strain experiments combined with our considerations do not yield information about the specific nature of the coupling between filler particles and polymer matrix. However, the generally observed large contribution of the entanglements to the mechanical behavior favors the entanglement–bound rubber model (EBRM) to describe the effects of carbon black on filled rubber properties at high and low strain as postulated in ref 30. In this EBRM, the carbon black affects the rubber property through its effect on the effective cross-link density ν_f, which is controlled by the entangled bulk rubber with bound rubber in a transition zone between the highly immobilized and localized bound rubber and the mobile bulk rubber phases (Figure 2). Because a single molecule of bound rubber is likely to adsorb on several carbon black surface sites, the bound rubber is essentially immobile in this model.[30] Hence, the effective cross-link density ν_f is related to the mean number of entanglements formed between the tightly absorbed bound rubber and the bulk rubber far removed from the carbon black surface. This model is consistent with some recent structural investigations of carbon black filler rubbers based on NMR line-width analysis.[49] In these experiments direct evidence of motional cooperation between the tightly and more loosely bound polymer layers around the filler particles was found. Probably, the mechanism by which the bound polymer is removed with increasing temperature has typical Arrhenius character.

The connection between G_e decrease and bound rubber increase in filled rubbers can then be discussed in the EBRM as follows:

The constraint modulus G_e depends on the local polymer segment density according to eq 23. We restrict our discussion to the typical case $a = 2$ and obtain

$$\frac{G_e(\varphi\neq 0)}{G_e(\varphi=0)} = \left(\frac{n_s'}{n_s}\right)^2 \tag{26}$$

where $n_s = N_s/V$ and $n_s' = N_s'/V_p$. Here, N_s is the total number of chain units (statistical segments) in the unfilled network sample of volume V. The total number of units in the mobile polymer phase of volume $V_p = V - V_{cb} - V_{oil}$ of the filled network is $N_s' = N_s - N_{br}$. The carbon black volume is V_{cb}, and the volume of the plasticizer (processing oil) V_{oil} can be neglected. The number of units adsorbed in the immobilized bound rubber layer on the carbon black surface is denoted by N_{br}. Its relative amount is given by

$$\frac{N_{br}}{N_s} = 1 - \frac{n_s'}{n_s}\left(1 - \frac{V_{cb}}{V}\right) = 1 - \frac{n_s'}{n_s}(1-\varphi) \tag{27}$$

and yields together with eq 26 the expression

$$\frac{N_{br}}{N_s} = 1 - \left(\frac{G_e(\varphi)}{G_e(0)}\right)^{1/2}(1-\varphi) \tag{28}$$

Let us consider the example of polybutadiene rubber. Table I yields $G_e(50\text{ phr cb})/G_e(0) = 0.85$ where 50 phr cb corresponds to the volume fraction $\varphi \approx 0.2$. Hence, we obtain $N_{br}/N_s \approx 0.26$; i.e., approximately 25–30% of the polymer is adsorped in the immobilized bound rubber layer. This agrees fairly well with direct estimations of the bound rubber amount in 50 phr filler vulcanizates.[30] It has to be realized that the bound rubber layer volume itself is small compared to the filler volume.

So far no clear and unique mechanism for formulation of bound rubber has been suggested. Several possibilities do not seen to be appropriate, as we will discuss below. It is assumed that reactive groups (acidic groups, phenolic groups, quinonic groups, and lactone groups have all been identified by specific reactions) on the carbon black surface influence adsorption; i.e., some sites between bound rubber molecules and the carbon black surface are likely to form

covalent bonds.[23,28,50] These conclusions agree with the picture of a highly energetically heterogeneous carbon black surface which is composed of a small fraction of high-energy sites surrounding a relative low-energy background.[63] This quantum chemistry picture alone underestimates possibly stronger effects induced by surface topography and physical adsorption (e.g., "weak" van der Waals bonds) that play an important role in understanding polymer attachment on disordered or even fractal surfaces. So far, this point has been completely ignored and a more detailed discussion will be given below.

Obviously, carbon black belongs to the class of porous surface fractal materials where neither the solid medium nor the pore space is fractal but the particles, the aggregates, and hence the pores within the aggregates have a fractal surface.[51] Zerda et al. found experimentally by BET techniques (gas adsorption on a surface) that the fractal surface dimension for carbon black particles is $D_f = 2.2 \pm 0.1$, and it is practically independent of the grade of the sample.[52] The fractal nature of surfaces can be determined and characterized by adsorbing molecules of different diameter. Pfeifer et al. have shown that the number of molecules required to cover the surface with a monolayer is given by $N = Sa^{-D_f}$, where a is the diameter of adsorbents, S is the Haudsdorff measure of the surface, and D_f is the fractal dimension of the surface.[53] D_f may vary between 2 and 3 (for a Euclidean surface, $D_f = 2$ and S is the usual (Euclidean) surface area). Bound rubber is then a consequence of strong surface irregularity measured by the fractal dimension. The amount of bound rubber increases with increasing surface irregularity. Already simple models contain the statement that increasing the surface irregularity shows the effect that the number of polymer–surface interactions is strongly enhanced relative to the idealized planar (regular) surface.[54] This is a consequence of a larger probability of polymer–surface intersection with increasing roughness. It can also be argued that adsorption occurs more readily on fractal surfaces since adsorption then requires a smaller entropic penalty.[54] Polymer adsorption occurs when the enthalpic contribution of attractive polymer–surface contacts overcomes the loss of configurational entropy arising from confinement to the surface. As a consequence, a rough surface may adsorb a polymer even if the corresponding smooth surface with the same adsorption energy of the same material will not favor adsorption of the molecule. Roughness alters the effective polymer–surface interaction in a fundamental way. Very recently, first attempts were made to understand the effect of polymer adsorption on rough surfaces more deeply.[55] In all cases, the basic physical origin of the criterion of adsorption of polymer chains is the competition between the gain in potential energy obtained by the polymer units by binding to the surface and the loss in chain entropy associated with the reduction in the number of possible chain configurations in comparison with that of free chains. Douglas et al. proposed an approximate expression by a Flory estimate for a critical polymer–surface interaction u_i on hypercubic lattices of dimension d and variable surface dimension D_f: $\exp(u_i/k_BT) = q(\text{free})/q(\text{confined}) \approx 2d/(d + D_f)$.[56] q(free) is the coordination number of the free chain in the absence of a surface, and q(confined) is the effective coordination number of a confined chain. We obtain with $d = 3$ and the fractal dimension of carbon black surface $D_f = 2.2$ the following ratio: $u_i(D_f=2.2)/u_i(D_f=2) \approx 0.785$. The results indicate that an increase of roughness decreases u_i. This is just a statement that a chain has to lose less configurational entropy to adsorb onto a rough surface. Thus, by roughening a surface, it may be even possible to convert a repulsive interface into an adsorbing interface without modifying the chemical "makeup" of the surface.[54] In contrast to covalent bonding effects between a polymer chain and carbon black surface, the disorder-induced localization effect acts on all segments of the chain.

We finally discuss some conclusions which can be drawn from the constraint modulus G_e. We already noted that this quantity is related to the lateral dimension of the configurational tubes within the bulk rubber (eq 17). A decrease of G_e with increasing filler content leads therefore to an increasing tube diameter d_o, i.e., a weakening of the configurational constraints.

An analytic expression for d_o has been given in eq 24. The values of the prefactor α_{nw} therein were estimated according to eq 25. They can be used to calculate explicitely the tube parameters for the unfilled networks. We given an impression for the numerical value of d_o in the case of high *cis*-polybutadiene networks. As relevant molecular parameters, the values $l_s = 0.76$ nm for the average length of the statistical segment and $M_s = 105$ g/mol for its molecular mass are used.[60] Then it follows that $n_s l_s^3 = \rho_P N_A l_s^3/M_s = 2.3$ (polymer density $\rho_P = 0.91$ g/cm^3; N_A is Avogadro's number) and d_o(unfilled) = $3.92(2.3)^{-1/2} \times 0.76$ nm ≈ 1.97 nm. Otherwise, the root-mean-square end-to-end distance of a network chain is given by $R_c = (M_c/M_s)^{1/2} l_s = (8481/105)^{1/2} \times 0.76$ nm $\approx$ 6.8 nm. The corresponding d_o values of the styrene–butadiene copolymer networks depend on the definition and the amount of the mean statistical steps lengths and molecular masses, respectively, which are not known precisely. Using composition data given here and defining a number-average length and a weight-average mass of the units, one obtains $d_o \approx 4.1$ and 2.7 nm for the high styrene–butadiene copolymer and high vinyl styrene–butadiene copolymer networks, respectively. These values, together with the values in ref 6 for natural rubber and PDMS networks, indicate that in all cases the tube diameters of moderately cross-linked elastomers are smaller than in the melt case (Table II) because cross-links give additional contributions to the constraining potential. With the typical relation $(n_s l_s^3)^{1/2} \gtrsim 1$, one finds then values of d_o somewhat larger than the statistical segment lengths l_s of the polymers. Stress–strain investigations of cross-linked emulsion styrene–butadiene copolymers with 23% styrene content (SBR 1500) and solution styrene–butadiene copolymers of varying styrene and vinyl content confirmed these findings.[57,61] We remark that the estimated length scale d_o is only 1 order larger than the nearest neighbor distance of polymer segments in the rubber. We find in all cases that the following relation, which agrees with the theoretical prediction, holds: $l_s < d_o < R_c$.[6,36,37] Additionally, the network is characterized by the typical relation $b_{PR} \approx l_s$.

The tube diameter increases slightly in the filled network because the constraint modulus G_e of the mobile polymer phase decreases ($n_s \rightarrow n_s' = n_s[G_e(\text{filled})/G_e(\text{unfilled})]^{1/2}$).

We note that the estimated moduli G_c and G_e change somewhat if the filled test specimens are first subjected to a number of deformation cycles (Mullins effect). Otherwise, the typical relations between the characteristic length scales do not change. These effects were investigated by the authors.[61] Carbon black filled samples of different polymers (emulsion as well as solution SBRs) were first subjected to nine deformation cycles (200% elongation) to destroy the carbon black networking and to minimize the influence of the carbon black/carbon black interaction on the stress–strain curve. We found a

somewhat larger effect on the modulus G_c—and, hence on the length scale R_c—than on the constraint modulus G_e or the tube parameter d_0. The estimated average end-to-end distance of the network chains, R_c, increases; e.g., for SBR 1500 filled with 50 phr carbon black from 3.9 to 4.7 nm, and the estimated tube scale decreases from 3.8 to 3.3 nm. The increase of R_c is related to a decrease of G_c, which is a result of the partially destroyed carbon black networking.[46] The slight decrease of d_0 (or increase of the modulus G_e) is still unclear. We may speculate that this effect is connected with a slight increase of the local segment number density within the mobile rubber phase at the expense of the segment density within the bound rubber and transition layer.

We finally note that the tube diameter is determined by the "van der Waals" diameter θ of the polymer chains. Using a unique correlation $d_c \approx 13.6\theta$ between the critical end-to-end distance for entanglements of flexible and semiflexible chains, d_c, and the average polymer chain diameter, one finds with $d_0 = d_c/(2)^{1/2}$ the correlation $d_0 \approx 10\theta$.[58] The average polymer chain diameter θ is estimated from the cross-sectional area of the polymer obtained from crystallographic data and from molecular modeling simulations.

4. Conclusions

(A) In conclusion we can say that the quasistatic mechanical properties of carbon black filled elastomers depend strongly on the number of elastically effective polymer–polymer cross-links, the lateral tube dimension in the mobile polymer phase, and the elastically effective number of polymer–filler junctions.

(B) Simple uniaxial stress–strain experiments, combined with a configurational constraining tubelike network theory, can be used as a simple method to estimate these three quantities together with the relationship between filled network parameters and static mechanical properties of the vulcanizates.

(C) The configurational tube diameter of unfilled and filled rubbers does not differ remarkably.

(D) The decrease of the constraint modulus of the filled network, relatively to its value of the unfilled network, led us to the conclusion that entanglements act between a tightly adsorbed bound layer and the mobile rubber removed from a fractal carbon black surface.

(E) The tube diameters estimated yield the mean numbers of statistical segments N_e between two successive entanglements in the mobile polymer phase: $N_e = d_0^2/l_s^2$. This number is a key quantity for the molecular prediction of the viscoelastic properties of filled elastomers.[47]

Acknowledgment. G.H. acknowledges Continental AG for permission to publish this paper.

Appendix

The following calculation of the free energy of filled networks is a rigorous generalization of the Deam–Edwards theory.[33]

The expression eq 2 is too complicated to do the functional integrations via the Greens function method because of the nonlocal form of the potential and also the $n + 1$ differential equations for the Greens functions are coupled. This difficulty is surmounted by employing a unitary transform (UT) on the $n + 1$ coordinates $\mathbf{R}^{(\alpha)}$ and $\mathbf{R}_c^{(\alpha)}$ to single out the "center of mass" coordinates $\mathbf{r}^{(0)}(s)$, $\mathbf{r}_c^{(0)}$ from the relative variables $\mathbf{r}^{(1)}(s)$, $\mathbf{r}^{(2)}(s)$, ..., $\mathbf{r}^{(n)}(s)$, etc., of the $(N + 1)$th system. The UT has the property that the expression for $Z(n)$ is unchanged. We may then argue that the potential term Q^* = eq 8b can be modeled by harmonic potential terms coming from all the $\mathbf{r}^{(\alpha)}$ variables except the center of mass variable:

$$-\frac{l_s}{6}\sum_{\alpha=1}^{n}\sum_{\mu}\int_0^L w_\mu^2 r_\mu^{(\alpha)2}(s)\,ds \tag{A.1}$$

with

$$w_\mu^2 = (w_\mu^c)^2 + (w_\mu^f)^2 \tag{A.2}$$

The quantity w_μ^2 is the strength of the harmonic potential, with two contributions coming from polymer–polymer cross-links and polymer–filler interaction. Then, the partition function takes the form

$$Z(n) = \oint\frac{d\mu_c M_c!}{2\pi i \mu_c^{M_c}}\oint\frac{d\mu_f M_f!}{2\pi i \mu_f^{M_f}}\int_{V^{(0)}}\cdots\int_{V^{(n)}}\delta\mathbf{r}^{(0)}(s)\cdots\delta\mathbf{r}^{(n)}(s)\times \exp\left\{-\frac{3}{2l_s}\sum_{\alpha=0}^{n}\int_0^L \dot{\mathbf{r}}^{(\alpha)}(s)^2\,ds - \frac{l_s}{6}\sum_{\alpha=1}^{n}\sum_{\mu}\int_0^L w_\mu^2 r_\mu^{(\alpha)}(s)^2\,ds + Q\right\} \tag{A.3}$$

where

$$Q = Q^* + \frac{l_s}{6}\sum_{\alpha=1}^{n}\sum_{\mu}\int_0^L w_\mu^2 r_\mu^{(\alpha)}(s)^2\,ds \tag{A.4}$$

The functional integrals are now directly integrable using the Greens functions G_α, which are given by the solutions of the corresponding differential equations.[33]

$$Z(n) = \oint\frac{d\mu_c M_c!}{2\pi i \mu_c^{M_c}}\oint\frac{d\mu_f M_f!}{2\pi i \mu_f^{M_f}}\times \int_{V^{(0)}}\cdots\int_{V^{(n)}}\prod_{\alpha=0}^{n}G_\alpha\,d\mathbf{r}^{(\alpha)}(0)\,d\mathbf{r}^{(\alpha)}(L)e^{Q} \tag{A.5}$$

The solutions for $G_{\alpha\neq 0}$ are

$$G_\alpha = \prod_\mu\left(\frac{w_\mu}{2\pi}\right)^{1/2}\exp\left\{-\frac{1}{2}w_\mu r_\mu^{(\alpha)2} - \frac{1}{2}w_\mu r_\mu^{f(\alpha)2} - \frac{l_s}{6}w_\mu L\right\} \tag{A.6}$$

for large L where the ground-state eigenfunctions dominate. The function G_0 is the solution of a "free diffusion equation" inside a box of the replicated box $V\prod_\mu(1 + n\lambda_\mu^2)^{1/2}$ with V the volume of the network sample and λ_μ the principal deformation ratios. The choice of cyclic boundary conditions gives

$$G_0 = \frac{1}{l_s\prod_\mu(1 + n\lambda_\mu^2)^{1/2}V} + \left(\frac{3}{2\pi l_s|s - s'|}\right)^{3/2}\times \exp\left\{-\frac{3}{2l_s}\frac{(\mathbf{r}^{(0)} - \mathbf{r}'^{(0)})^2}{|s - s'|}\right\} \tag{A.7}$$

where the first term is the constant part due to mean density of chains and the second term is due to the enhanced probability of finding a single chain. The choice of the cyclic boundary conditions allows the calculation to proceed with the uniform density condition that in reality is imposed by molecular forces, such as excluded-volume interactions.[33] To complete the calculation we

use the usual Feynman variational principle; i.e., a best and constant value C for Q will be chosen so as to give a lower bound for $Z(n)$ and thus an upper bound for the free energy $F(n)$.[59] Writing

$$Q \rightarrow C + (Q - C)$$

we have

$$\langle e^{Q-C} \rangle \geq 1 + \langle Q - C \rangle \tag{A.8}$$

and find the best value of C when $C = \langle Q \rangle$. Thus

$$Z(n) \geq \oint \frac{d\mu_c M_c!}{\mu_c^{M_c+1}} \oint \frac{d\mu_f M_f!}{\mu_f^{M_f+1}} e^{\langle Q \rangle} \psi(n) \tag{A.9}$$

$$\psi(n) = \prod_{\alpha=0}^{n} \int\int d\mathbf{r}_0^{(\alpha)}\, d\mathbf{r}_L^{(\alpha)} G_\alpha(\mathbf{r}_0, \mathbf{r}_L; \mathrm{OL}) \tag{A.10}$$

with the following results:

$$\psi(n) = V \prod_\mu (1 + n\lambda_\mu^2)^{1/2} \left(\frac{w_\mu}{2\pi}\right)^{-n/2} \times \exp\left(-\frac{n l_s L}{6} w_\mu\right) \tag{A.11}$$

$$\langle Q \rangle = \mu_c \langle Q_1 \rangle + \mu_f \langle Q_2 \rangle + \langle Q_3 \rangle \tag{A.12}$$

$$\langle Q_1 \rangle = \frac{L^2}{V} \prod_\mu (1 + n\lambda_\mu^2)^{-1/2} \left(\frac{w_\mu}{2\pi}\right)^{n/2} \tag{A.13}$$

$$\langle Q_2 \rangle = \frac{L^k}{V^{k-1}} \prod_\mu (1 + n\lambda_\mu^2)^{-(k-1)/2} \left(\frac{w_\mu}{\pi}\right)^{(k-1)n/2} \times \varphi_\mu^{n(k-1)} k^{-n/2} \tag{A.14}$$

where $k = f_F/2$.

$$\varphi_\mu = \left(1 + \frac{1}{2} w_\mu \epsilon_\mu^2\right)^{1/2} \tag{A.15}$$

$$\langle Q_3 \rangle = \sum_\mu \frac{n l_s L}{12} w_\mu \tag{A.16}$$

We find from eqs A.14 and A.15

$$\lim_{\epsilon_\mu \to 0} \langle Q_2 \rangle = \langle Q_1 \rangle \quad \text{for} \quad k = 2 \; (f_F = 4) \tag{A.17}$$

That is, the filler particle of zero diameter acts as a conventional cross-linking point. In this case, the results take the form of the original DE phantom network theory.

Inserting of $\psi(n)$ and $\langle Q \rangle$ into eq A.9 and performing the pole integration by steepest decent, one obtains

$$Z(n) \geq \exp\{M_c \log \langle Q_1 \rangle + M_f \log \langle Q_2 \rangle - \langle Q_3 \rangle + \text{const}\} \tag{A.18}$$

and thus with eq 1

$$\frac{F}{k_B T} \leq \frac{1}{2}(M_c + g_f M_f) \sum_\mu \lambda_\mu^2 - \frac{M_c}{2} \times \sum_\mu \ln\left(\frac{w_\mu}{2\pi}\right) - \frac{g_f M_f}{2} \sum_\mu \ln\left(\frac{w_\mu}{\pi}\right) + \frac{g_f M_f}{2} \times \sum_\mu \ln\left(1 + \frac{1}{2}\epsilon_\mu^2 w_\mu\right) + \sum_\mu \frac{l_s L}{12} w_\mu + \frac{3}{2} \ln k \tag{A.19}$$

with $g_f = k - 1 = (f_F - 2)/2 \approx f_F/2$ for $f_F \gg 1$.

The best values for the parameter w_μ are determined by minimizing the free energy. The equation

$$\partial F / \partial w_\mu = 0 \tag{A.20}$$

yields for undeformable fillers ($\epsilon_x = \epsilon_y = \epsilon_z = \epsilon$) the solution

$$w_\mu = w = \frac{1}{\epsilon^2}\left(\frac{w^c \epsilon^2}{2} - 1\right) \times \left\{\left(1 + \frac{12(M_c + g_f M_f)}{N l_s L'} \frac{\epsilon^2}{\left(1 - \frac{w^c \epsilon^2}{2}\right)^2}\right)^{1/2} - 1\right\} \tag{A.21}$$

which is independent of deformation λ_μ. Here, N is the number of primary chains of contour length L'. The quantity

$$w^c = 6M_c/(N l_s L') = 6M_c/(N_c l_s L_c) \tag{A.21}$$

is the solution for the unfilled network case $M_f = 0$ (L_c is the contour length of the network chain between two chemical cross-links). We note that eq A.21 simplifies for $w^c \epsilon^2/2 = 3M_c \epsilon^2/(N_c l_s L_c) \gg 1$ and gives

$$w \approx 2/\epsilon^2 \tag{A.22}$$

The condition is fulfilled in the normal case of moderately cross-linked ($M_c/N_c = 2/f$; f is the functionality of cross-links) polymer phases in filled vulcanizates where $\epsilon^2 \gg l_s L_c$, i.e., filler dimensions $\gg$ network chain dimensions. Equation A.19 and the deformation-independent quantity A.21 lead then to the elastic free energy expression eq 9.

References and Notes

(1) Kästner, S. *Faserforsch. Textiltech./Z. Polymerforsch.* **1976**, *27*, 1; *Colloid Polym. Sci.* **1981**, *259*, 499, 508.
(2) Ronca, G.; Allegra, G. *J. Chem. Phys.* **1975**, *63*, 4990.
(3) Flory, P. J. *J. Chem. Phys.* **1977**, *66*, 5720. Erman, B.; Flory, P. J. *J. Chem. Phys.* **1978**, *68*, 5363. Flory, P. J.; Erman, B. *Macromolecules* **1982**, *15*, 800.
(4) Gottlieb, M.; Gaylord, R. J. *Polymer* **1983**, *24*, 1644. Higgs, P. G.; Gaylord, R. J. *Polymer* **1990**, *31*, 70.
(5) Batsberg, W.; Kramer, O. *J. Chem. Phys.* **1981**, *74*, 6507. Kramer, O. *Kautsch, Gummi, Kunstst.* **1987**, *40*, 109. Twardowski, T.; Kramer, O. *Macromolecules* **1991**, *24*, 5769. Kramer, O. Information on the Role of Chain Entangling Obtained by Crosslinking in the Strained State. In *Elastomeric Polymer Networks*; Mark, J. E., Erman, B., Eds.; Prentice Hall: Englewood Cliffs, NJ, 1992; p 243.
(6) Heinrich, G.; Straube, E.; Helmis, G. *Adv. Polym. Sci.* **1988**, *85*, 33.
(7) Vilgis, T. A. Polymer Networks. In *Comprehensive Polymer Science*; Pergamon Press: Oxford, England, 1989; Vol. 6.
(8) Oppermann, W.; Rennar, N. *Prog. Colloid Polym. Sci.* **1987**, *75*, 49.
(9) Matzen, D.; Straube, E. *Colloid Polym. Sci.* **1992**, *270*, 1.
(10) Straube, E.; Heinrich, G. *Kautsch. Gummi, Kunstst.* **1991**, *44*, 734.
(11) Douglas, J. F.; McKenna, G. B. The Localization Model: Review and Extension to Swollen Rubber Elasticity. In *Elastomeric Polymer Networks*; Mark, J. E., Erman, B., Eds.; Prentice Hall: Englewood Cliffs, NJ, 1992; p 327; McKenna, G. B.; Gaylord, R. J. *Polymer* **1988**, *29*, 2027.
(12) Kästner, S. *Colloid Polym. Sci.* **1981**, *259*, 508. Erman, B.; Monnerie, L. *Macromolecules* **1989**, *22*, 3342.
(13) Graessley, W. W. *Adv. Polym. Sci.* **1982**, *47*, 67.
(14) Doi, M.; Edwards, S. F. *J. Chem. Soc., Faraday Trans. 2* **1978**, *74*, 1789, 1802, 1818; **1979**, *75*, 38.
(15) Kosc, M. *Colloid Polym. Sci.* **1988**, *266*, 105.
(16) Higgs, P. G.; Ball, R. C. *Europhys. Lett.* **1989**, *8*, 357.
(17) Adolf, D. *Macromolecules* **1988**, *21*, 228.
(18) Edwards, S. F.; Vilgis, T. A. *Polymer* **1986**, *27*, 483.
(19) Edwards, S. F.; Vilgis, T. A. *Rep. Prog. Phys.* **1988**, *51*, 243.
(20) Ball, R. C.; Doi, M.; Edwards, S. F.; Warner, M. *Polymer* **1981**, *22*, 1010.
(21) Marrucci, G. *Macromolecules* **1981**, *14*, 434. Gaylord, R. J. *Polym. Bull.* **1982**, *8*, 325. Gaylord, R. J.; Douglas, J. F. *Polym. Bull.* **1987**, *18*, 347; **1990**, *23*, 529.
(22) Kraus, G. *Adv. Polym. Sci.* **1971**, *8*, 155.

(23) Donnet, J. B.; Vidal, A. *Adv. Polym. Sci.* **1986**, *76*, 104.
(24) Medalia, A. J. *Rubber Chem. Technol.* **1972**, *45*, 1172.
(25) Dannenberg, E. M. *Rubber Chem. Technol.* **1975**, *48*, 410.
(26) Schikowsky, M. Theoretical Investigation of the Stress-Strain-Behavior of Carbon Black Filled Networks. Ph.D. Thesis, Technical University Merseburg, 1989 (in German).
(27) Edwards, D. C. *J. Mater. Sci.* **1990**, *25*, 4175.
(28) Häusler, K. G.; Heinrich, G.; Schikowsky, M.; Straube, E.; Stepto, R. F. T. *Acta Polym.* **1991**, *42*, 169.
(29) Medalia, A. J. *J. Colloid Interface Sci.* **1970**, *32*, 115.
(30) Funt, J. M. *Rubber Chem. Technol.* **1988**, *61*, 842.
(31) Gerspacher, M.; O'Farrell, C. P.; Yang, H. H. *Elastomerics* **1990**, (Nov), 23. Gerspacher, M.; O'Farrell, C. P. *Elastomerics* **1991**, (April), 35. Gerspacher, M.; Yang, H. H. *Caoutch. Plast.* **1990**, *No. 696*, 206.
(32) Schikowsky, M. Diploma Thesis, Technical University Merseburg, 1984 (in German).
(33) Deam, R. T.; Edwards, S. F. *Philos. Trans. R. Soc. A* **1976**, *280*, 317. Deam, R. T. The Free Energy of a Phantom Chain Network. In *Molecular Fluids*; Balian, R., Weill, G., Eds.; Gordon and Breach: New York, 1976.
(34) Parisi, G. Statistical Mechanics of Amorphous Systems. In *Proceedings, Les Houches Summer School. Recent Advances in Field Theory and Statistical Mechanics*; Zuber, J. B., Stora, R., Eds.; North Holland: Amsterdam, 1984.
(35) Bueche, A. M. *J. Polym. Sci.* **1957**, *25*, 139.
(36) Heinrich, G.; Straube, E. *Acta Polym.* **1983**, *34*, 589; **1984**, *35*, 115.
(37) Heinrich, G.; Straube, E. *Polym. Bull.* **1987**, *17*, 247.
(38) Edwards, S. F. *Proc. Phys. Soc.* **1967**, *92*, 9. Edwards, S. F. *J. Phys. C* **1969**, *2*, 1.
(39) Doi, M.; Edwards, S. F. *Theory of Polymer Dynamics*; Oxford University Press: Oxford, England, 1986.
(40) Graessley, W. W.; Edwards, S. F. *Polymer* **1981**, *22*, 1329.
(41) Colby, R. H.; Rubinstein, M.; Viovy, J. L. *Macromolecules* **1992**, *25* 996.
(42) Roovers, J.; Toporowski, P. M. *Rubber Chem. Technol.* **1990**, *63*, 734.
(43) Heinrich, G.; Straube, E. *Makromol. Chem., Makromol. Symp.* **1989**, *30*, 223.
(44) Butera, R.; et al. *Phys. Rev. Lett.* **1991**, *66*, 2088.
(45) Helmis, G.; Heinrich, G.; Straube, E. *Wiss. Z. Tech. Hochsch. Leuna-Merseburg* **1984**, 26, 461.
(46) Eisele, U.; Mueller, H.-K. *Kautsch. Gummi, Kunstst.* **1990**, *43*, 9.
(47) Heinrich, G. *Kautsch. Gummi, Kunstst.* **1992**, *45*, 173. Heinrich, G.; Rennar, N.; Stähr, J. *Kautsch. Gummi, Kunstst.* **1992**, *45*, 442.
(48) Straube, E.; Matzen, D. *Kautsch. Gummi, Kunstst.* **1992**, *45*, 264. Matzen, D. The Reinforcement of SBR-Compounds and Networks with Carbon Black. Ph.D. Thesis, Technical University Merseburg, 1989 (in German).
(49) Kenny, J. C.; McBrierty, V. J.; Rigbi, Z.; Douglass, D. C. *Macromolecules* **1991**, *24*, 436.
(50) *Reinforcement of Elastomers*; Kraus, G., Ed.; John Wiley: New York, 1965.
(51) Gouyet, J.-F.; Rosso, M.; Sapoval, B. Fractal Surfaces and Interfaces. In *Fractals and Disordered Systems*; Bunde, M., Havlin, S., Eds.; Springer-Verlag: Berlin, 1991.
(52) Zerda, T. W.; Young, H.; Gerspacher, M. 139th Meeting of the Rubber Division, American Chemical Society, Toronto, ON, Canada, May 21–24, 1991.
(53) Pfeifer, P.; Avnir, D. *J. Chem. Phys.* **1983**, *79*, 3558. Pfeifer, P.; Farin, D.; Avnir, D. *J. Chem. Phys.* **1983**, *79*, 3566.
(54) Douglas, J. F. *Macromolecules* **1989**, *22*, 3707.
(55) Edwards, S. F.; Chen, Y. *J. Phys. A* **1988**, *21*, 2963. Blund, M.; Barford, W.; Ball, R. *Macromolecules* **1989**, *22*, 1458. Baumgärtner, A.; Muthukumar, M. *J. Chem. Phys.* **1991**, *94*, 4062.
(56) Douglas, J. F.; Nemirovsky, A. M.; Freed, K. F. *Macromolecules* **1986**, *19*, 2041.
(57) Heinrich, G., unpublished results.
(58) Zang, Y. H.; Carreau, P. J. *J. Appl. Polym. Sci.* **1991**, *42*, 1965.
(59) Feynman, R. P.; Hibbs, A. R. *Path Integrals and Quantum Mechanics*; McGraw-Hill: New York, 1965.
(60) Aharoni, S. M. *Macromolecules* **1986**, *19*, 426.
(61) Heinrich, G.; Vilgis, T. A. *Kautsch. Gummi, Kunstst.*, submitted. Heinrich, G.; Vilgis, T. A. Proceedings, 4th European Polymer Federation Symposium on Polymeric Materials, Baden-Baden, Germany, Sept 27–Oct 02, 1992; p 246. Heinrich, G., unpublished results.
(62) Heinrich, G.; Beckert, W. *Prog. Colloid Polym. Sci.* **1992**, *90*, 47.
(63) Donnet, J. B.; Lansinger, C. M. *Kautsch. Gummi, Kunstst.* **1992**, *45*, 459.
(64) Flory, P. J. *Proc. R. Soc. London* **1976**, *A351*, 351.
(65) Christensen, R. M. *Mechanics of Composite Materials*; J. Wiley & Sons Inc.: New York, 1979.